Research Article | Vol. 26, No. 16 | 6 Aug 2018 | OPTICS EXPRESS 21033
Optics EXPRESS

Frequency domain diffuse optical spectroscopy with a near-infrared tunable vertical cavity surface emitting laser

VINCENT J. KITSMILLER,[1] MATTHEW M. DUMMER,[2] KLEIN JOHNSON,[2] GARRETT D. COLE,[3] AND THOMAS D. O'SULLIVAN[1,*]

[1]*University of Notre Dame, Dept. of Electrical Engineering, Notre Dame, IN 46556, USA*
[2]*Vixar Inc., 2950 Xenium Ln N #104, Plymouth, MN 55441, USA*
[3]*Advanced Optical Microsystems, 1243 West El Camino Real, Mountain View, CA 94040, USA*
[*]*tosullivan@nd.edu*

Abstract: We present an approach for performing frequency domain diffuse optical spectroscopy (fd-DOS) utilizing a near-infrared tunable vertical cavity surface emitting laser (VCSEL) that enables high spectral resolution optical sensing in a miniature format. The tunable VCSEL, designed specifically for deep tissue imaging and sensing, utilizes an electrothermally tunable microelectromechanical systems topside mirror to tune the laser cavity resonance. At room temperature, the laser is tunable across 14nm from 769 to 782nm with single mode CW output and a peak output power of 1.3mW. We show that the tunable VCSEL is suitable for use in fd-DOS by measuring the optical properties of a tissue-simulating phantom over the tunable range. Optical properties were recovered within 0.0006mm^{-1} (absorption) and 0.09mm^{-1} (reduced scattering) compared to a broadband fd-DOS reference system. Our results indicate that tunable VCSELs may be an attractive choice to enable high spectral resolution optical sensing in a wearable format.

OCIS codes: (140.3600) Lasers, tunable; (140.7260) Vertical cavity surface emitting lasers; (230.4685) Optical microelectromechanical devices; (170.6510) Spectroscopy, tissue diagnostics; (170.3660) Light propagation in tissues.

References and links

1. B. Pogue, M. Testorf, T. McBride, U. Osterberg, and K. Paulsen, "Instrumentation and design of a frequency-domain diffuse optical tomography imager for breast cancer detection," Opt. Express **1**(13), 391–403 (1997).
2. A. T. Eggebrecht, S. L. Ferradal, A. Robichaux-Viehoever, M. S. Hassanpour, H. Dehghani, A. Z. Snyder, T. Hershey, and J. P. Culver, "Mapping distributed brain function and networks with diffuse optical tomography," Nat. Photonics **8**(6), 448–454 (2014).
3. L. A. Coldren, G. A. Fish, Y. Akulova, J. S. Barton, L. Johansson, and C. W. Coldren, "Tunable semiconductor lasers: a tutorial," J. Lightwave Technol. **22**(1), 193–202 (2004).
4. P. Qiao, K. T. Cook, K. Li, and C. J. Chang-Hasnain, "Wavelength-swept VCSELs," IEEE J. Sel. Top. Quantum Electron. **23**(6), 1700516 (2017).
5. I. Grulkowski, J. J. Liu, B. Potsaid, V. Jayaraman, J. Jiang, J. G. Fujimoto, and A. E. Cable, "High-precision, high-accuracy ultralong-range swept-source optical coherence tomography using vertical cavity surface emitting laser light source," Opt. Lett. **38**(5), 673–675 (2013).
6. V. Jayaraman, G. D. Cole, M. Robertson, C. Burgner, D. John, A. Uddin, and A. Cable, "Rapidly swept, ultra-widely-tunable 1060 nm MEMS-VCSELs," Electron. Lett. **48**(21), 1331–1333 (2012).
7. C. Gierl, T. Gruendl, P. Debernardi, K. Zogal, C. Grasse, H. A. Davani, G. Böhm, S. Jatta, F. Küppers, P. Meissner, and M.-C. Amann, "Surface micromachined tunable 1.55 μm-VCSEL with 102 nm continuous single-mode tuning," Opt. Express **19**(18), 17336–17343 (2011).
8. T. D. O'Sullivan, K. No, A. Matlock, R. V. Warren, B. Hill, A. E. Cerussi, and B. J. Tromberg, "Vertical-cavity surface-emitting laser sources for gigahertz-bandwidth, multiwavelength frequency-domain photon migration," J. Biomed. Opt. **22**(10), 1–8 (2017).
9. B. Pezeshki, J. S. Harris Jr.,"Electrostatically tunable optical device and optical interconnect for processors," US07939903 (1992).
10. THORLABS, "1300 nm MEMS VCSEL Swept Laser Source," https://www.thorlabs.com/newgrouppage9.cfm?objectgroup_id=7109.
11. B. Kogel, A. Abbaszadehbanaeiyan, P. Westbergh, A. Haglund, J. Gustavsson, J. Bengtsson, E. Haglund, H. Frederiksen, P. Debernardi, and A. Larsson, "Integrated tunable VCSELs with simple MEMS technology," in

#331210 https://doi.org/10.1364/OE.26.021033
Journal © 2018 Received 9 May 2018; revised 12 Jul 2018; accepted 22 Jul 2018; published 31 Jul 2018

Optics EXPRESS

22nd *IEEE International Semiconductor Laser Conference*, Kyoto, pp. 1–2 (2010).
12. H. A. Davani, C. Grasse, B. Kögel, C. Gierl, K. Zogal, T. Gründl, P. Westbergh, S. Jatta, G. Bohm, P. Meissner, A. Larsson, and M. C. Amann, "Widely electro thermal tunable bulk-micromachined MEMS-VCSEL operating around 850nm," in *2011 Int. Quantum Electron. Conf., IQEC 2011 and Conf. Lasers and Electro-Optics, CLEO Pacific Rim 2011 Incorporating the Australasian Conf. Optics, Lasers and Spectroscopy and the Australian Conf.*, pp. 32–34.
13. Y. Zhou, M. C. Huang, and C. J. Chang-Hasnain, "Tunable VCSEL with ultra-thin high contrast grating for high-speed tuning," Opt. Express **16**(18), 14221–14226 (2008).
14. P. Tayebati, P. Wang, D. Vakhshoori, C. C. Lu, M. Azimi, and R. N. Sacks, "Half-symmetric cavity tunable microelectromechanical VCSEL with single spatial mode," IEEE Photonic. Tech. Lett. **10**(12), 1679–1681 (1998).
15. G. D. Cole, E. Behymer, T. C. Bond, and L. L. Goddard, "Short-wavelength MEMS-tunable VCSELs," Opt. Express **16**(20), 16093–16103 (2008).
16. J. A. Lott, M. J. Noble, E. M. Ochoa, L. A. Starman, and W. D. Cowant, "Tunable red vertical cavity surface emitting lasers using flexible micro-electro-mechanical top mirrors," in *IEEE/LEOS International Conference on Optical MEMS.*, (Cat. No.00EX399), Kauai, HI, 2000, pp. 81–82.
17. C. C. Sthalekar and V. J. Koomson, "A CMOS sensor for measurement of cerebral optical coefficients using non-invasive frequency domain near infrared spectroscopy," Sensors Journal, IEEE **13**(9), 3166–3174 (2013).
18. B. Kogel, P. Westbergh, A. Haglund, J. S. Gustavsson, and A. Larsson, "Integrated MEMS-tunable VCSELs with high modulation bandwidth," Electron. Lett. **47**(13), 764–765 (2011).
19. G. D. Cole, E. S. Bjorlin, Q. Chen, C. -Yeung Chan, S. Wu, C. S. Wang, N. C. MacDonald, and J. E. Bowers, "MEMS-tunable vertical-cavity SOAs," IEEE J. Quantum Electron. **41**(3), 390–407 (2005).
20. V. Kitsmiller, M. Dummer, K. Johnson, and T. D. O'Sullivan, "Tunable vertical cavity surface emitting lasers for use in the near infrared biological window," in *Optical Fibers and Sensors for Medical Diagnostics and Treatment Applications XVIII*, I. Gannot, ed. (SPIE, 2018), **10488**, pp. 20.
21. B. J. Tromberg, L. O. Svaasand, T.-T. Tsay, R. C. Haskell, and M. W. Berns, "Optical property measurements in turbid media using frequency-domain photon migration," in L. O. Svaasand, ed. (International Society for Optics and Photonics, 1991), **1525**, 52–58.
22. T. D. O'Sullivan, A. E. Cerussi, D. J. Cuccia, and B. J. Tromberg, "Diffuse optical imaging using spatially and temporally modulated light," J. Biomed. Opt. **17**(7), 071311 (2012).
23. L. O. Svaasand and B. J. Tromberg, "Properties of optical waves in turbid media," in L. O. Svaasand, ed. (International Society for Optics and Photonics, 1991), **1525**, 41–51.
24. T. Vo-Dinh and B. R. Masters, Biomedical Photonics Handbook, (CRC Press, 2003), Chap. 22.
25. J. B. Fishkin, S. Fantini, M. J. vandeVen, and E. Gratton, "Gigahertz photon density waves in a turbid medium: Theory and experiments," Phys. Rev. E Stat. Phys. Plasmas Fluids Relat. Interdiscip. Topics **53**(3), 2307–2319 (1996).
26. R. C. Haskell, L. O. Svaasand, T.-T. Tsay, T.-C. Feng, M. S. McAdams, and B. J. Tromberg, "Boundary conditions for the diffusion equation in radiative transfer," J. Opt. Soc. Am. A **11**(10), 2727–2741 (1994).
27. A. E. Cerussi, R. Warren, B. Hill, D. Roblyer, A. Leproux, A. F. Durkin, T. D. O'Sullivan, S. Keene, H. Haghany, T. Quang, W. M. Mantulin, and B. J. Tromberg, "Tissue phantoms in multicenter clinical trials for diffuse optical technologies," Biomed. Opt. Express **3**(5), 966–971 (2012).
28. A. Leproux, T. D. O'Sullivan, A. Cerussi, A. Durkin, B. Hill, N. Hylton, A. G. Yodh, S. A. Carp, D. Boas, S. Jiang, K. D. Paulsen, B. Pogue, D. Roblyer, W. Yang, and B. J. Tromberg, "Performance assessment of diffuse optical spectroscopic imaging instruments in a 2-year multicenter breast cancer trial," J. Biomed. Opt. **22**(12), 121604 (2017).
29. J. A. Lott, M. J. Noble, E. M. Ochon, L. A. Starman, and W. D. Cowan, "Tunable red vertical cavity surface emitting lasers using flexible micro-electro-mechanical top mirrors," in *2000 IEEE/LEOS International Conference on Optical MEMS (Cat. No.00EX399)* (IEEE, n.d.), pp. 81–82.
30. A. E. Cerussi, K. Conde, J. Lam, and V. Verma, "Broadband characterization of tissue simulating phantoms using a supercontinuum laser in a scanning diffuse optical spectroscopy instrument," in B. J. Tromberg, A. G. Yodh, E. M. Sevick-Muraca, and R. R. Alfano, eds. (SPIE, 2015), **9319**, 93191Z.
31. J. Wang, S. C. Davis, S. Srinivasan, S. Jiang, B. W. Pogue, and K. D. Paulsen, "Spectral tomography with diffuse near-infrared light: inclusion of broadband frequency domain spectral data," J. Biomed. Opt. **13**(4), 041305 (2008).
32. A. Bassi, J. Swartling, A. Pifferi, A. Torricelli, R. Cubeddu, and C. D'Andrea, "Time-resolved spectrophotometer for turbid media based on supercontinuum generation in a photonic crystal fiber," Opt. Lett. **29**(20), 2405–2407 (2004).
33. S. Konugolu Venkata Sekar, A. Dalla Mora, I. Bargigia, E. Martinenghi, C. Lindner, P. Farzam, M. Pagliazzi, T. Durduran, P. Taroni, A. Pifferi, and A. Farina, "Broadband (600-1350 nm) time-resolved diffuse optical spectrometer for clinical use," IEEE J. Sel. Top. Quantum Electron. **22**(3), 7100609 (2016).
34. S. H. Chung, A. E. Cerussi, C. Klifa, H. M. Baek, O. Birgul, G. Gulsen, S. I. Merritt, D. Hsiang, and B. J. Tromberg, "In vivo water state measurements in breast cancer using broadband diffuse optical spectroscopy," Phys. Med. Biol. **53**(23), 6713–6727 (2008).
35. S. Kukreti, A. E. Cerussi, W. Tanamai, D. Hsiang, B. J. Tromberg, and E. Gratton, "Characterization of metabolic differences between benign and malignant tumors: high-spectral-resolution diffuse optical

Optics EXPRESS

spectroscopy," Radiology **254**(1), 277–284 (2010).
36. K. M. Blackmore, J. A. Knight, R. Jong, and L. Lilge, "Assessing breast tissue density by transillumination breast spectroscopy (TIBS): an intermediate indicator of cancer risk," Br. J. Radiol. **80**(955), 545–556 (2007).

1. Introduction

Noninvasive diffuse optical imaging and sensing in deep living tissue is technologically constrained by the commercial availability of miniature light sources in the first near-infrared biological optical window (NIR-I, ~650-1350nm). Adding spectral content and source channels to diffuse optical imaging instruments – typically in the form of additional lasers or LEDs – can increase accuracy and expand the number of detectable chromophores, but at the expense of increased size and complexity. This tradeoff is readily apparent in the development of diffuse optical tomography instruments for breast [1] or brain [2] imaging, wherein increasing spatial and spectral sampling of the tissue can improve 3D spatial resolution, sensitivity, and chromophore discrimination. Concurrently, there is a competing desire to reduce the size of these devices to enable handheld and wearable sensing, illustrating the need for a miniature near-infrared tunable light source.

Electrically-pumped, tunable monolithic semiconductor lasers are well-suitable for this application because of their narrow (instantaneous) spectral linewidth, favorable power efficiency, and high modulation bandwidth for time and frequency domain techniques, all in a robust sub-millimeter package. Tunable devices that have been produced include single and arrayed distributed feedback (DFB) lasers, single and multi-section distributed Bragg reflector (DBR) lasers [3], and tunable vertical-cavity surface-emitting lasers (VCSELs) [4–7]. Of these options, a tunable VCSEL is desirable because its inherent short optical cavity lends itself to continuous tuning via a simple mechanism (i.e. changing the cavity length), as opposed to the complex mode selection required for the other lasers. Furthermore, because of their small size and diverse low-cost packaging options, VCSELs are attractive optical sources for wearable sensors and multi-channel systems in which size and scalability are important [8]. While tunable VCSELs have been investigated for nearly 25 years [9], only within the last few years have VCSEL-based swept sources become widely commercially available. As of this writing, commercial tunable VCSELs are only available for wavelengths above 1μm [10], though shorter wavelength devices have been demonstrated by multiple groups [11–16].

In this paper, we report on the design, fabrication, and implementation of a short wavelength tunable VCSEL for performing frequency domain diffuse optical spectroscopy (fd-DOS) of tissue in the NIR-I window. fd-DOS and the related time-domain diffuse optical spectroscopy (i.e., via the temporal Fourier transform) are methods that perform quantitative tissue optical spectroscopy by measuring both the optical absorption and scattering coefficients of living biological tissue. fd-DOS has been investigated for multiple clinical applications [17], and our group and others are developing wearable sensors that integrate this approach [8]. Integration of a compact tunable source with sufficient modulation bandwidth can greatly increase spectral information in a compact device without negatively affecting size or complexity.

Like other tunable VCSELs, continuous optical tuning of our device is accomplished by displacing a suspended top mirror utilizing a microelectromechanical systems (MEMS) structure to adjust the optical cavity length. However, unlike electrostatically driven MEMS mirrors actuated with electrostatic forces that require 10's of volts to operate, this mirror operates with less than 1V, making it a practical and attractive source for compact microelectronic and battery-powered systems. The applied tuning current induces ohmic heating that causes the mirror support beams to expand and displace the suspended MEMS mirror, similar to the designs seen in [7,11,12,18]. Importantly, our monolithically integrated approach is compatible with standard wafer-scale VCSEL fabrication and is therefore readily translatable to high volume production.

Optics EXPRESS

This paper is organized as follows. In Section 2, we describe the design of the NIR-I tunable MEMS-VCSEL device and, in Section 3, we discuss the fd-DOS technique and its optical source requirements. Section 4 contains our results and discussion including the optical and electronic performance of the tunable VCSEL and fd-DOS optical property measurements of a tissue-simulating phantom over the tunable range of the tunable VCSEL. Finally, we conclude and describe future research directions in Section 5.

2. Tunable VCSEL design

Our tunable VCSEL consists of the monolithic integration of a half VCSEL structure—bottom distributed Bragg reflector (DBR) and quantum well active region—with a suspended dielectric MEMS microlens mirror that can be displaced vertically with electrothermal actuation [Fig. 1]. The bottom DBR mirror and multi-quantum well active region were grown on GaAs wafers utilizing metal-organic chemical vapor deposition (MOCVD). The bottom DBR consists of more than 40 alternating n-doped AlGaAs layer pairs to achieve a reflectivity of greater than 99.9% over a free spectral range of 35nm. Ion implantation below the topside annular p-type contact defines the current aperture. An antireflective coating lies above the active region to dampen coupled cavity effects between the semiconductor and airgap and also aides in linearizing wavelength tuning [19].

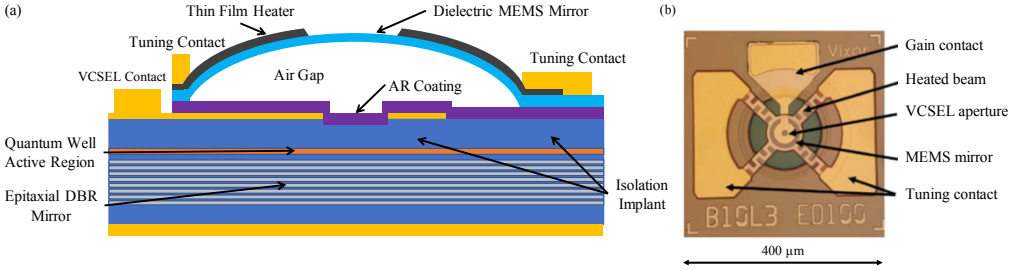

Fig. 1. Structure of NIR wavelength GaAs/AlGaAs based tunable VCSEL with electrothermally actuated monolithically integrated topside MEMS mirror. (a) Cross section diagram of device structure. (b) Topside photograph of a typical fabricated device.

The topside MEMS-tunable dielectric mirror is a curved microlens centered above the optical cavity. The center reflective region is supported by 4 beams also composed of the same dielectric material. Thin film heating elements with a resistance of approximately 100 ohms were patterned across the supporting arms to facilitate electrothermal tuning. We designed a curved microlens so that mirror displacement would be symmetric across the optical field and minimize diffractive loss. Current is supplied to tuning contacts on either side of the mirror, which is dissipated as heat into the mirror. This causes thermal expansion of the dielectric and increases the airgap height. Cooling via convection allows the mirror to return to its initial state. Fabrication of the MEMS mirror is described in detail in [20]. Briefly, a sacrificial layer was deposited on the half-VCSEL epitaxial layers and etched into the microlens shape utilizing a reflowed photoresist mask. The dielectric mirror was blanket deposited over the sacrificial lens. Cantilever supports were patterned in the dielectric via photolithography and etched with RIE to expose the underlying sacrificial lens material. The heating elements and bonding pads were deposited and patterned with a lift-off technique. Finally, the sacrificial layer was removed using an isotropic dry etch to create the air gap. No critical point drying was required. At this point the tunable mirror was free standing and fabrication of the device was complete.

3. Frequency-domain diffuse optical spectroscopy (fd-DOS)

fd-DOS is a model-based measurement technique used to quantify the optical properties—absorption and reduced scattering coefficients—of a turbid medium and has been widely

Optics EXPRESS

explored for use in noninvasive biomedical imaging [20–22]. In this method, the attenuation and retardation of a photon density wave (PDW) created by intensity-modulated light that propagates through a sample is captured at a photoreceiver [23]. PDW propagation in multiple-scattering media is well-described by the time-dependent radiative transport equation (RTE) for photons which relates absorption and scattering coefficients to the relative amplitude and phase of the source and detected signals [24–26]. Therefore, fitting the measured amplitude and phase of the detected PDW in an appropriate frequency range—typically 50-1000MHz—to the RTE can provide quantitative estimates of the sample' optical properties. This process can be performed at multiple optical wavelengths in order to assess the wavelength dependent absorption and scattering properties of the sample and to extract further meaningful information such as chromophore concentrations in tissue. This technique allows noninvasive characterization of tissue up to several centimeters deep and can also be utilized for diffuse optical tomography.

Suitable sources for fd-DOS must be capable of outputting several milliwatts of optical power and be capable of intensity modulation up to 1 GHz. After we assessed these device characteristics (results in section 4), we integrated the tunable VCSEL into a fd-DOS system, seen in Fig. 2, and measured the optical properties of a silicon-based tissue-simulating optical phantom [27]. DC current from a laser driver (LDC-3916370, ILX Lightwave, Bozeman, Montana) was combined with RF power provided by a network analyzer (8753ES, HP/Agilent, Santa Clara, California) using a bias tee and injected into the VCSEL. The output power was fiber coupled (400μm core diameter multimode fiber) and brought into contact with the surface of the silicone tissue simulating phantom. The resulting PDW was measured using a 1mm diameter active area avalanche photodiode (APD) module (S12060-10/C5658, Hamamatsu Corp., Shizuoka Japan) which was in direct contact with the phantom. Output from the APD module was sent to the network analyzer which captures phase and amplitude of the PDW relative the source excitation. Calibration, which accounts for instrument response, was carried out on a separate tissue simulating phantom with known optical properties. Measured phase and amplitude data was fit to a P1 approximation to the RTE with semi-infinite boundary conditions using the Levenberg-Marquardt algorithm which yielded estimates of the phantom absorption and reduced scattering coefficients [25,26].

These measurements were compared to a broadband fd-DOS system that utilizes a combination of laser diodes and a tungsten halogen lamp to measure broadband NIR optical properties. The design and operation of the reference system, which was replicated and validated in a multi-center clinical study of breast cancer response to chemotherapy is described in references [28].

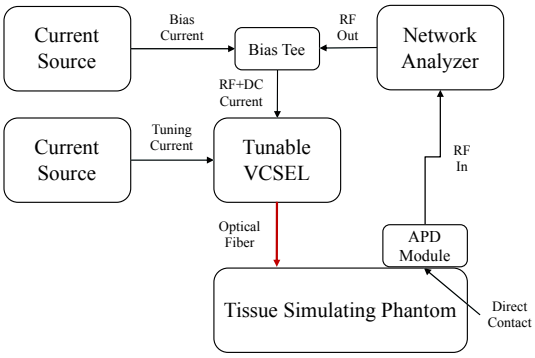

Fig. 2. fd-DOS system configuration with a tunable VCSEL. RF power and DC bias current are combined with a bias tee and used to bias the VCSEL. An additional current source is used to provide tuning current to the VCSEL. Optical power is delivered to a tissue simulating phantom with an optical fiber. The APD module collects the signal and returns it to the network analyzer for magnitude and phase determination.

Optics EXPRESS

4. Results and discussion

4.1 Optical power and tuning range

All electrical and optical characterization of the tunable VCSELs were performed under continuous wave operation at room temperature without temperature control. All data was taken from segmented and packaged (TO46-5 cans) die with 8μm diameter aperture and 300μm diameter mirror. Figure 3(a) shows that the VCSEL's peak lasing wavelength is tunable across 769-782nm for a total 14nm range. The device is continuously tunable across this range, and the peak output wavelength is linear with respect to the electrical power supplied to the tuning contacts [Fig. 3(b)]. The VCSEL lases at tuning currents from 5 to 11mA, which corresponds to applied tuning voltages ranging from 425 to 935mV. Spectra observed on an optical spectrum analyzer across the 14nm tuning range show single longitudinal mode operation and side mode suppression of more than 15dBm, which was limited by the noise floor of the measurement.

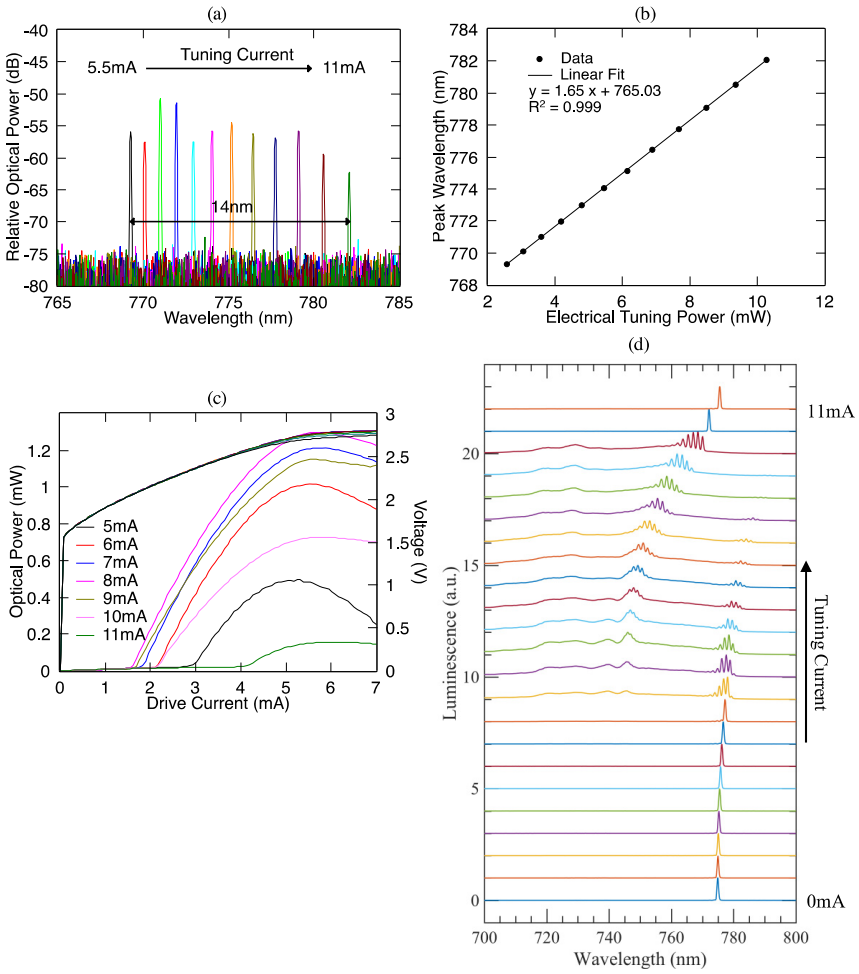

Fig. 3. Performance of 775nm electrothermally actuated tunable VCSELs with applied tuning current. (a) Spectra taken across the tunable lasing wavelength range. (b) Wavelength tuning as a function of electrical tuning power in the MEMS DBR mirror. (c) Optical power and voltage versus current across the lasing range. (d) Normalized electroluminescence measurements across the full tuning range (0-11mA in 0.5mA steps) showing adjacent cavity resonances and the free spectral range of 32nm. Note (d) is a different device shown in (a)-(c).

Optics EXPRESS

Peak optical power depends upon the tuning wavelength, as shown in the current-voltage and optical power curves in Fig. 3(c). A peak power of 1.3mW at 774nm was achieved near the middle of the tuning range with 8mA tuning current applied. This also corresponded to the lowest threshold current of 1.6mA. This phenomenon is observed because this operation point corresponds closely with the design wavelength (775nm) where decisions were made to maximize gain minus loss (e.g. overlap between optical mode and quantum well gain region, mirror reflectivity, etc.) Furthermore, optimal tuning current differed between devices due to variation in the morphology of the top mirror (further discussed below).

Free spectral range (FSR) of the tunable laser cavity was determined by recording the electroluminescence spectra as a function of tuning current slightly above lasing threshold [Fig. 3(d)] utilizing a spectrometer (AvaSpec-Mini, Avantes, Apeldoorn Netherlands) coupled to a reflectance microscope. The adjacent cavity resonances are clearly visible at tuning currents between 5 and 8 mA. The narrow spectra corresponded to lasing conditions, while the spectra indicated by multiple oscillations were subthreshold and may have been due to additional transverse modes in the laser cavity. The latter point needs further investigation for confirmation. The FSR was determined to be 32nm which is close to the designed 35nm. The data indicates that the optical cavity is tunable across the entire FSR, however, lasing only occurred near the long wavelength edge. In this particular device, which is a separate device than the one characterized in Fig. 3(a)-3(c), lasing occurred again at higher tuning currents at the short wavelength end as the second cavity resonance was shifted toward the gain spectrum.

The VCSEL beam profile was examined using a quartz diffuser as an imaging plane with known height above the VCSEL and imaged with a CCD camera. This device had a full width at half maximum beam divergence of 13.2° in one direction and 6.9° in the perpendicular direction and operated in a higher order transverse mode at all tuning wavelengths. Transverse modal behavior was variable between devices; other devices lased at different higher order modes and exhibited mode hopping during tuning. We believe that the devices did not operate in a single transverse mode because the mirror etch was unexpectedly anisotropic, resulting in a microlens curvature that was not symmetric. The asymmetric mirror structure led to lasing of higher order transverse modes.

Although the 14nm tuning range and 1.3mW peak optical power of our device is comparable to other tunable VCSELs emitting at less than 1μm [13,29], it fell short of our performance expectations. We believe both of these performance issues were due to higher than expected optical loss in the VCSEL structure, and lower quantum well gain at the short wavelengths. Specifically, scanning electron microscopy of the tunable mirror (not shown) show obvious surface roughness, which in addition to the previously discussed asymmetry, causes optical scattering and loss. Furthermore, the top metal contact created an aperture that resulted in a small step on the deposited dielectric mirror, causing additional optical loss. We plan to rectify these issues in subsequent designs.

Importantly, we were able to achieve this tuning range with a tuning voltage of less than 1V, which is comparable to those seen in other electrothermal devices (1.2-1.6V) [7,11] and is much lower than tuning voltages required for electrostatically tuned devices (~20V) [13–15,29].

4.2 Tuning speed

The VCSEL tuning speed was characterized by applying triangular wave current injection across the tuning contacts (6221, Keithley/Tektronix, Beaverton Oregon) and measuring the above threshold optical output with a near-infrared spectrometer (AvaSpec-Mini, Avantes, Apeldoorn Netherlands). Since the period of the triangle wave (10-4000 Hz) was much smaller than the spectrometer integration time (400ms / 2.5Hz) the measurement yielded a time average of relative optical power as a function of wavelength [Fig. 4(a)]. We expected that as the mirror could not mechanically respond (thermally) to the changing tuning current,

Optics EXPRESS

the overall tuning range should be reduced. The mirror frequency response is described by a first order low pass filter obeying the relation [7]:

$$\delta\lambda = \frac{\delta\lambda_0}{\sqrt{1+(2\pi f\tau)^2}}, \quad (1)$$

where $\delta\lambda$ is the tuning range (nm), $\delta\lambda_0$ is the maximum tuning range (nm), f is the tuning current frequency (Hz), and τ is the thermal time constant (s) associated with the mirror. We see in Fig. 4(b) that the mirror was capable of tuning at speeds up to 500Hz without significant loss of tuning range. At 1kHz the tuning range was observed to reduce to 12nm and, at the maximum tested tuning frequency of 4kHz, the tuning range was reduced to 8nm. Reduction in tuning range is a result of the inability of the mirror dielectric to expand or relax in response to changes in tuning current. For this reason, the mirror experiences a loss of tuning range and simply responds as if an average tuning current was applied. Therefore, the tuning range narrows, but remains centered at the middle of the full tunable range as the frequency of the tuning current increases. Fitting of tuning frequency versus tuning range data to Eq. (1) yields a fitted maximum tuning range of 13.5nm which agrees well with our static tuning range [i.e. Fig. 3(a)] of 14nm and a thermal time constant of 46μs.

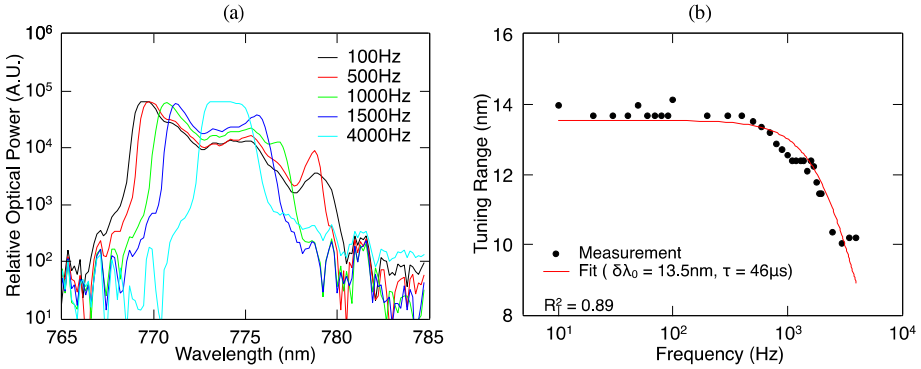

Fig. 4. VCSEL tuning speed characteristics. (a) Continuous wavelength tuning over tuning frequencies up to 4kHz. (b) 14 nm tuning range is achievable up to a frequency of approximately 500Hz. At the maximum tested tuning frequency of 4KHz the tuning range is reduced to 10nm.

We define the tuning speed as the product of tuning range and tuning range frequency (before tuning range begins to decrease, i.e. the maximum 0dB frequency). The tuning speed of our device is therefore 5464 nm/s, which is approximately twice as fast compared to devices utilizing a thermal tuning mechanism which have tuning speeds of 2400 and 2610nms^{-1} respectively [7,12]. This tuning speed is however much slower than speeds obtained with electrostatically tuned high contrast gratings 16000nms^{-1} [13], as would be expected due to the faster tuning mechanism given the inherent bandwidth advantages in electrostatic actuation coupled with the low mass of the suspended grating mirror.

4.3 Modulation efficiency

Modulation frequency response of the VCSEL was investigated by applying sinusoidal modulation utilizing a network analyzer (TR1300, Copper Mountain Technologies, Indianapolis Indiana) combined with a 5mA DC offset current via a bias tee. Laser output power as a function of frequency was observed with a photodiode (DET025AFC, Thorlabs, Newton New Jersey) [Fig. 5(a)]. We measured a 3dB bandwidth greater than 650MHz, which is sufficient for frequency domain diffuse optical spectroscopy (fd-DOS). The VCSEL's

Optics EXPRESS

modulation efficiency ε, defined as $\varepsilon = 1 - V_{max} / V_{min}$, where V_{max} is the maximum detector voltage and V_{min} is the minimum detector voltage, was investigated as a function of frequency, Fig. 5(b). When the RF power was fixed at the power to achieve maximum modulation depth at 50MHz, we see that the efficiency diminishes linearly from approximately 100% at 50MHz to below 40% at 1GHz. However, when the RF power was increased as a function of frequency, efficiency can be maintained above 85% up to a modulation of 1GHz. This data is consistent with a previous study of commercially available non-tunable VCSEL modulation efficiency wherein the authors found that modulation efficiency can be maintained above 90% up to 1GHz modulation frequencies when RF power is increased as a function of frequency [8].

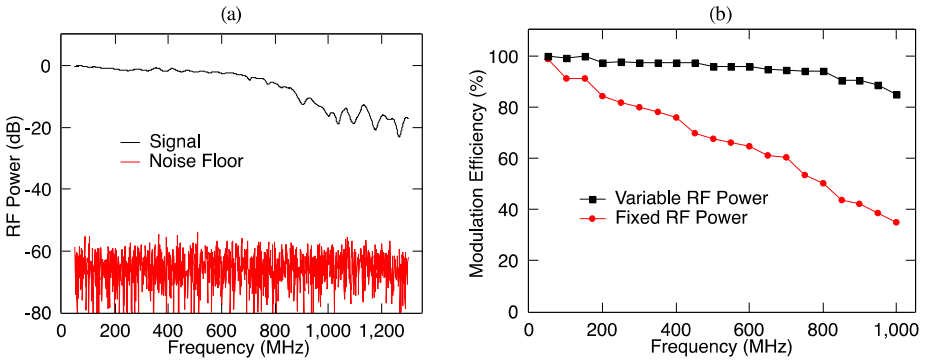

Fig. 5. VCSEL modulation characteristics. (a) The modulation bandwidth and (b) modulation efficiency for fixed and increasing RF injection power.

4.4 fd-DOS phantom measurement

Tissue-simulating phantom measurements were taken at a source/detector separation of 13mm with the VCSEL operating at peak power for each wavelength (between 0.4 – 1.2mW) and a fixed RF power of 10dBm from 50 to 500MHz. Figure 6(a) is representative calibrated fd-DOS amplitude and phase data for a single wavelength, which shows a good fit to the P1 semi-infinite model. Table 1 shows the results of 10 repeated tissue simulating phantom measurements at each wavelength. Recovered absorption and reduced scattering coefficients were within 0.0006mm^{-1} (absorption) and 0.09mm^{-1} (scattering) of the reference system across an 11nm tuning range [Fig. 6(b)]. The larger deviations were associated with the ends of the tuning range where lower output power resulted in a lower signal to noise ratio (SNR). The low output power of our tunable VCSELS currently limits the use of these devices to short source/detector separations (<15 mm) because of tissue optical attenuation.

Table 1. Tunable VCSEL Optical Property Recovery

Wavelength (nm)	Mean Absorption Coefficient (mm^{-1})[a]	Absorption Difference from Reference (%)	Mean Reduced Scattering Coefficient (mm^{-1})[a]	Scattering Difference from Reference (%)
769.6	0.0088	–2.4	0.909	–11.6
770	0.0090	–5.4	0.857	–5.2
771	0.0089	–7.0	0.810	0.5
772	0.0084	–4.3	0.769	5.5
773.5	0.0082	–6.3	0.768	5.6
775	0.0077	–4.6	0.750	7.7
777	0.0075	–7.7	0.739	9.0
779	0.0072	–9.7	0.754	7.1

[a]Standard deviations less than 0.00011mm^{-1} (absorption coefficient) and 0.0073mm^{-1} (reduced scattering coefficient)

Optics EXPRESS

We have previously shown that (single-wavelength) VCSELs are attractive for use as miniature optical sources in fd-DOS, particularly for wearable applications; they possess the output power and modulation efficiency necessary to recover deep tissue optical properties in vivo [8]. In this work, we see that tunable VCSELs are additionally capable of performing high spectral resolution spectroscopy with fd-DOS. Other approaches to achieve high spectral resolution tissue spectroscopy include utilizing large format tunable or supercontinuum fiber lasers [30–33] or by combining fd-DOS in a hybrid measurement with a broadband lamp and spectrometer [28]. However, these approaches are not amenable to miniaturization and are not easily scalable to multiple source channels. Based on our results here, we conclude that tunable VCSELs are promising to enable high spectral resolution measurements in ultra-small formats. Broadband tissue spectroscopy can reveal richer information content compared to typical approaches that use discrete wavelengths. Besides enabling estimation of additional chromophores (e.g., myoglobin, water, lipid, collagen) with greater accuracy, broadband methods can be used to assess the molecular state (protein-bound and free) and temperature of tissue water [34]. Broadband methods have also been shown to reveal specific absorption features that are unique to breast tumors [35] and characterize breast density [36].

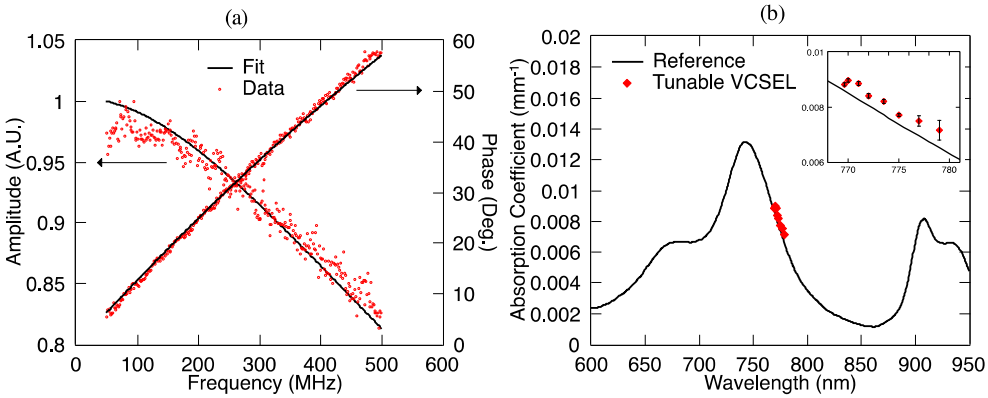

Fig. 6. fd-DOS measurements on a tissue-simulating phantom. (a) Representative amplitude and phase data from the tunable VCSEL as well as their associated P1 semi-infinite fits. (b) Comparison of the measured phantom optical properties between the tunable VCSEL and a reference broadband fd-DOS system.

5. Conclusion and future work

The advancement of diffuse optical imaging technologies for biomedical applications depends upon technological improvement in red and near infrared laser sources. Competing desires to decrease size, cost and increase scalability are typically at odds with the desire to increase functionality and information content. Furthermore, miniature sources are required for creating the next generation of wearable and implantable optical sensors. Overall, we have demonstrated that a monolithically integrated NIR VCSEL can be used to provide high spectral resolution tissue optical spectroscopy in a smaller footprint and at a potentially lower cost than larger format broadband approaches. The tunable VCSEL was shown to be suitable in fd-DOS measurements carried out on a tissue simulating phantom, in which optical properties were successfully recovered. Though the tuning range and optical power were lower than anticipated, we expect them to improve with optimization of the VCSEL design and microfabrication process. With these improvements, our ultimate goal is to achieve tunability across the NIR-I window by integrating multiple tunable VCSEL devices with separate center wavelengths into a single package.

Funding

National Institutes of Health (Grant No.: 5R44CA176848).

Optics EXPRESS

Acknowledgments

The authors acknowledge Dr. Patrick Fay, Dr. Anthony Hoffman, and Dr. Suman Datta for making their labs generously available to us, as well as Galen Hardin and Benjamin Grisafe for their aid. We also acknowledge the support of the Notre Dame Nanofabrication Facility.

The content of this proceeding does not necessarily reflect the position or policy of the Government, and no official endorsement should be inferred.